

Supplementary Figures and Supplementary Tables for

**Reprogramming the tumor immune microenvironment using
engineered dual-drug loaded *Salmonella***

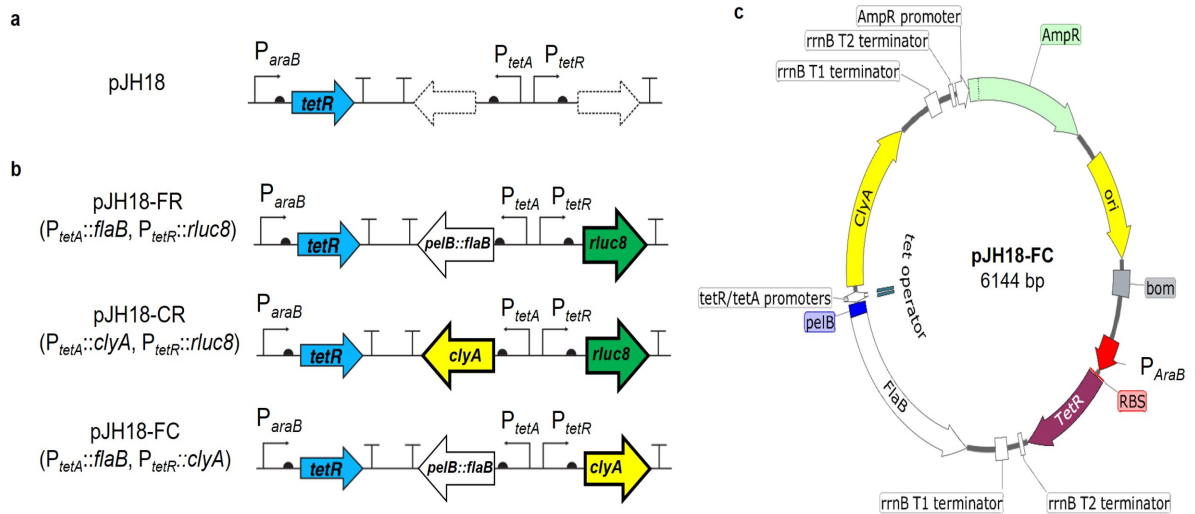
Dinh-Huy Nguyen *et al.*

***Corresponding authors:**

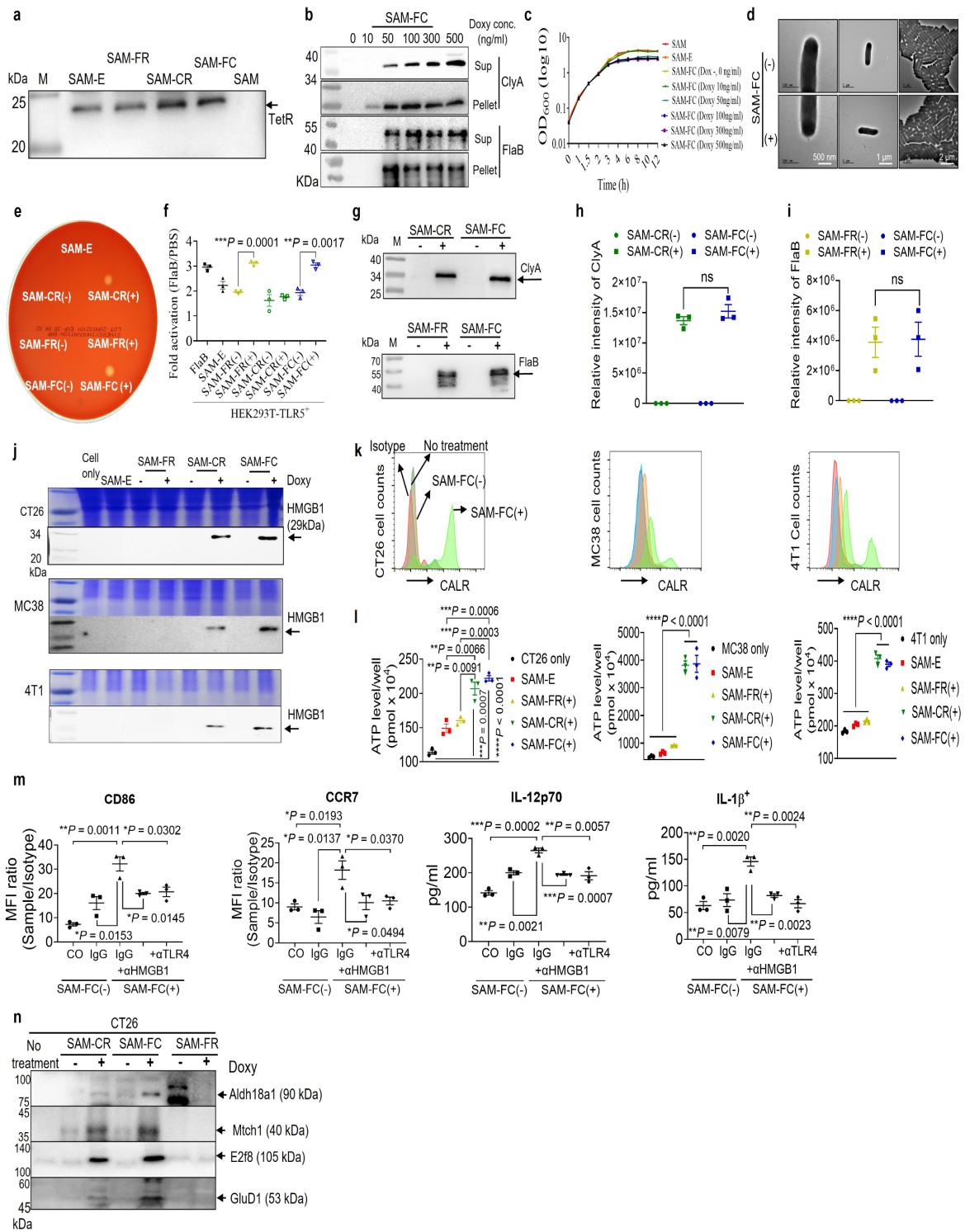
Jung-Joon Min (jjmin@jnu.ac.kr), Yeongjin Hong (yjhong@chonnam.ac.kr), and Sang-Jun Ha (sjha@yonsei.ac.kr)

This PDF file includes:

Supplementary Fig. 1 to 13
Supplementary Table 1 to 5

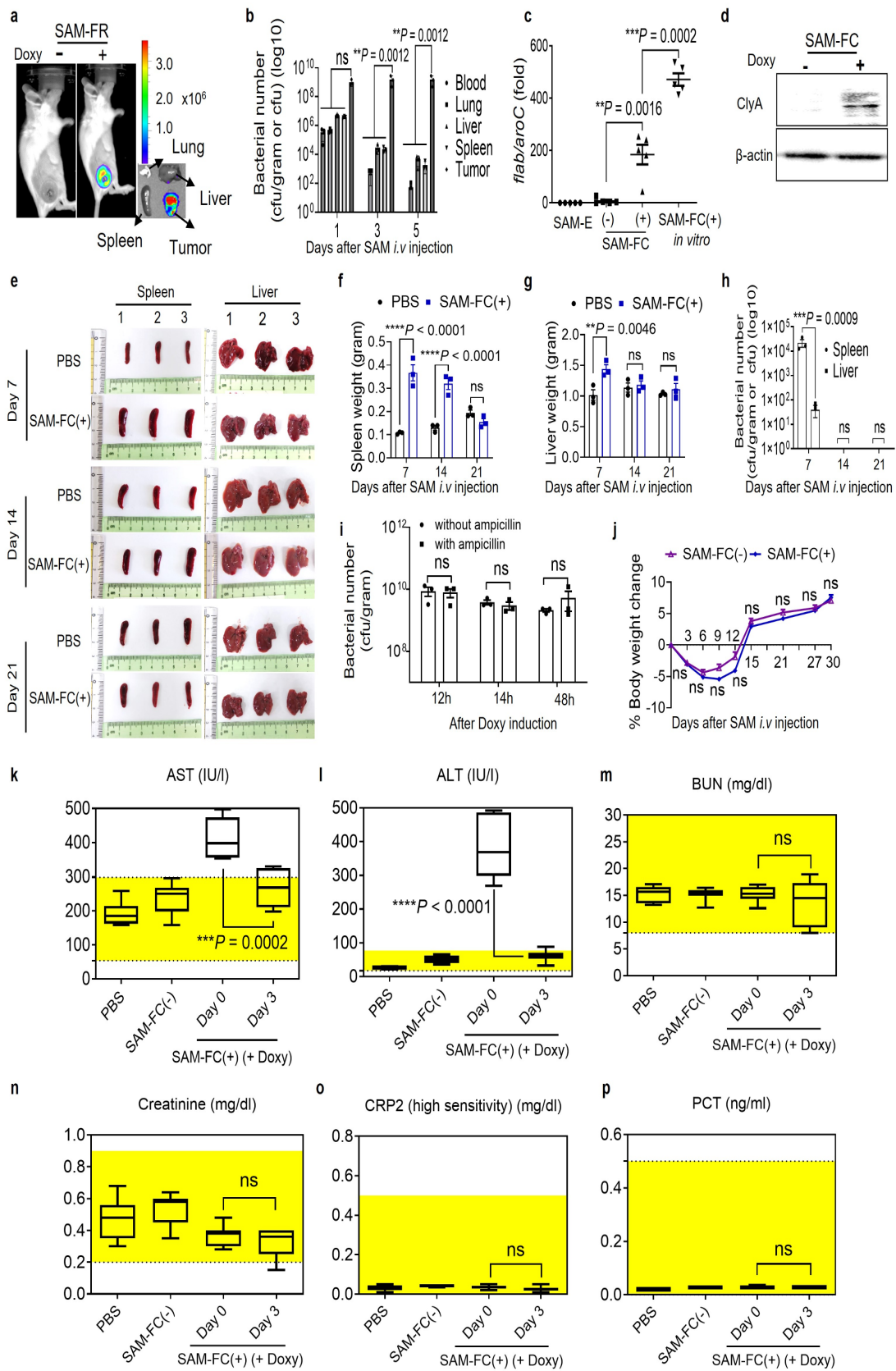


Supplementary Figure 1: Plasmids used in the study (related to Fig. 1a). **a** pJL87, the original plasmid used for SAM genetic engineering. The *tetR* gene, encoding a Doxycycline (Doxy)-binding transcription factor, is constitutively expressed via the P_{AraB} promoter. Tumor payload genes were inserted behind the P_{tetA} and P_{tetR} promoters (dotted arrows). **b** pJH18 plasmids carrying tumor payloads (pJH18-CR, pJH18-FR, and pJH18-FC), where C indicates *clyA*; R, *rluc8*; and F, *pelB::flaB*. **c** Full map of pJH18-FC. Amp^R, ampicillin resistance gene; ori, replication origin; RBS, ribosomal binding sites; *bom*, basis-of-mobility gene. Please also see Supplementary Table 1 and 2.



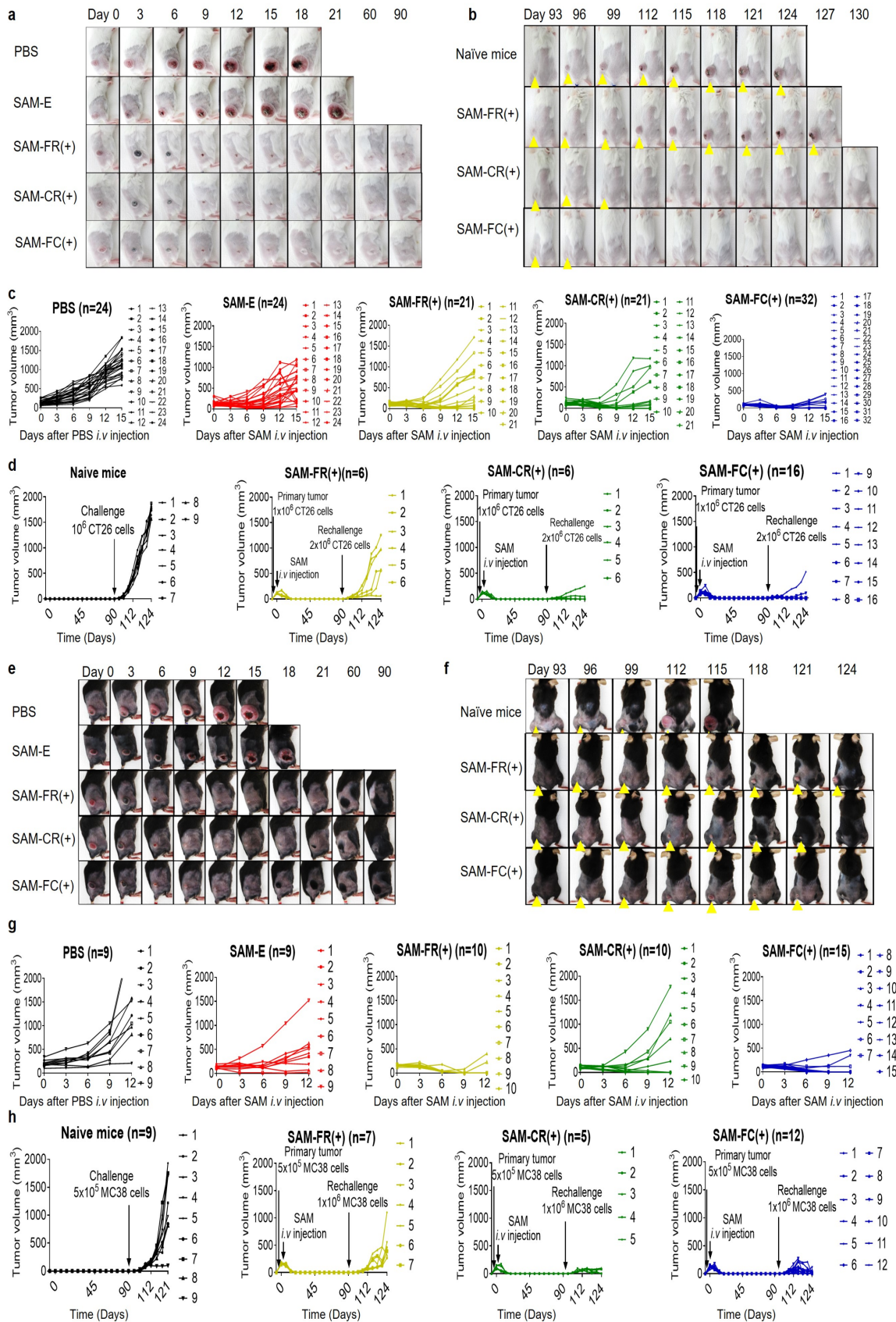
Supplementary Figure 2: Characterization of SAM-FC (related to Fig. 1a). **a** TetR expression in the absence of Doxy. TetR protein (~23 kDa) from transformed bacteria was detected with its specific antibody in western blot analysis. The untransformed bacteria (SAM) were used as a control. M, size marker. **b** Expression levels of ClyA and FlaB in SAM-FC bacteria by SDS-PAGE and western blotting with anti-ClyA (upper panels) and anti-FlaB (bottom panels) antibodies. **c** Growth of SAM-FC. Various concentrations of Doxy were added to bacterial subcultures at 0.5–0.7 OD₆₀₀ (0 h). The bacteria were then further cultured at 37°C. **d** Bacterial morphology of SAM-FC. The bacteria in the absence (-) or presence (+, 300 ng/ml) was collected after 4h and their morphologies were observed by transmission electron microscopy (TEM). **e** Activity of ClyA. -, without Doxy; +, with Doxy. **f** Functional assay of FlaB secreted from SAM-FC ($n = 3$ technical replicates; unpaired two-tailed t -

test). **g** Western blot images of SAM-FC, SAM-CR and SAM-FR expression. Quantification of **(h)** ClyA and **(i)** FlaB in **(g)** ($n = 3$ technical replicates; unpaired two-tailed t -test). **j** Western blot images of HMGB1 from tumor cells after treatment with the bacterial supernatant for 12h. **k** CALR translocation on the surface of tumor cells (CT26, MC38, and 4T1) treated with SAM-FC supernatants. The cells were stained with an anti-CARL antibody and analyzed by flow cytometry. **l** ATP release from CT26, MC38, or 4T1 cells after a 1 h treatment with SAM-E, SAM-FR, SAM-CR, or SAM-FC supernatants. The amount of ATP in the cell culture soup was measured using an ATP assay kit ($n = 3$ technical replicates; $**P = 0.0066$ [SAM-E vs SAM-CR(+)], $**P = 0.0091$ [SAM-FR(+) vs SAM-CR(+)], $***P = 0.0007$ [PBS vs SAM-CR(+)], $***P = 0.0006$ [SAM-E vs SAM-FC(+)], $***P = 0.0003$ [SAM-FR(+) vs SAM-FC(+)], and $****P < 0.0001$; unpaired two tailed t -test). **m** Maturation of BM-derived DCs induced by tumor cells treated with SAM-FC supernatant ($n = 3$ technical replicates; unpaired two tailed t -test). **n** Expression of tumor associated antigens (TAAs) in CT26 cells after treatment with SAM-FC supernatants.



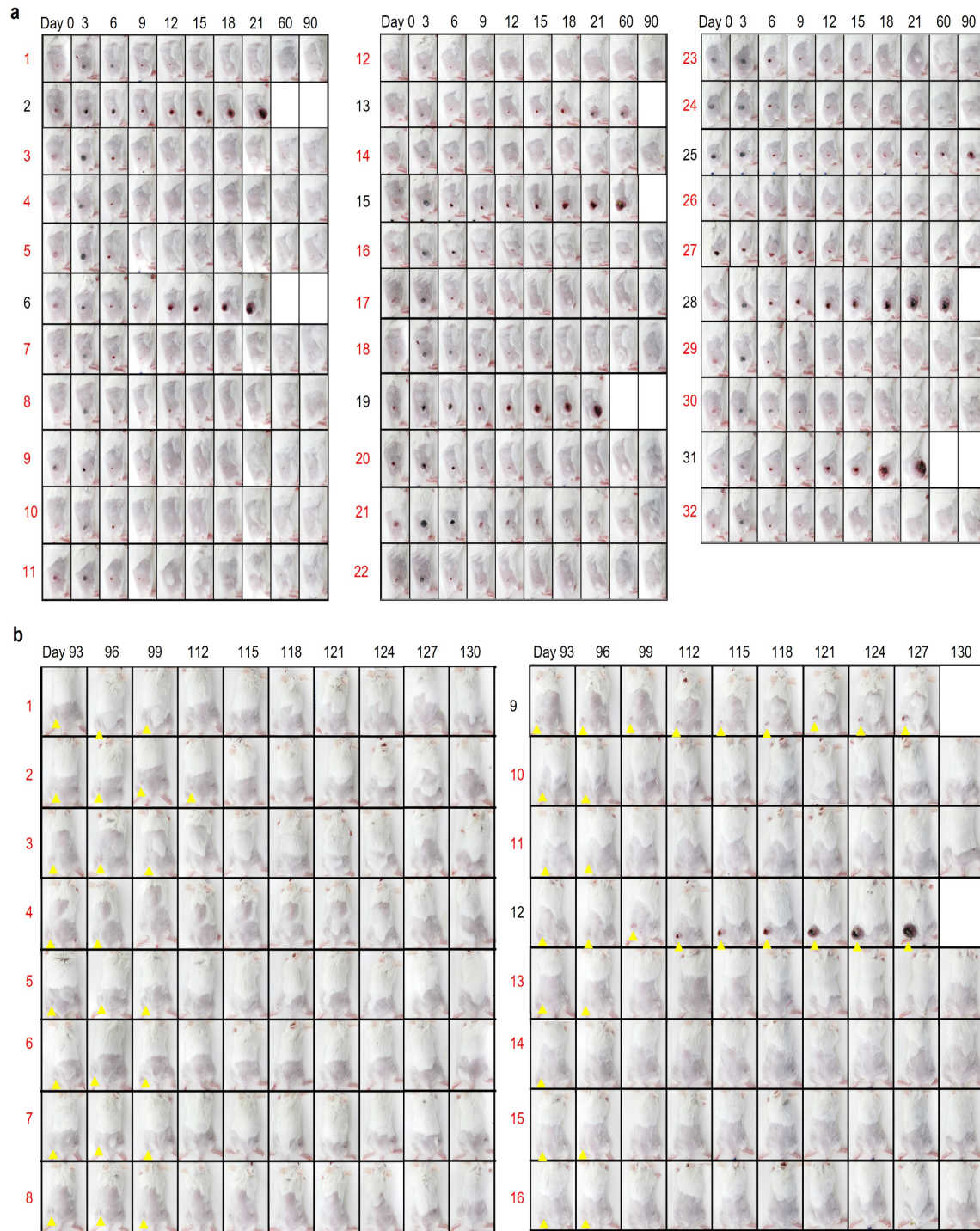
Supplementary Figure 3: Tumor targeting by engineered SAM bacteria in tumor-bearing mouse models. CT26 tumor-bearing BALB/c mice were injected intravenously with SAM-FR or SAM-FC (2×10^7 cfu), followed by oral administration of Doxy

daily starting on day 3 (a-h). The spleen and liver tissues were isolated to measure their weights and bacterial localization on day 7, 14, and 21. (-), without Doxy; (+), with Doxy. **a** Bioluminescence imaging of SAM-FR. The images were obtained after intravenous injection of coelenterazine (0.7 mg/kg) into mice treated with SAM-FR. **b** Biodistribution of SAM-FC ($n = 3$ mice/group, from one experiment; ns, not significant; two-way ANOVA with Tukey's multiple comparisons test). **c** Expression of *flaB* gene in tumors colonized by SAM-FC ($n = 5$ mice/group, from one experiment; unpaired two-tailed *t*-test). **d** Expression of the *clyA* gene in tumor tissues colonized by SAM-FC [SAM-FC(-) ($n = 3$) and SAM-FC(+) ($n = 5$), from one experiment]. Western blots were performed using anti-ClyA (upper panel) and anti- β actin (bottom panel) antibodies. **e** Images of spleens and livers. The weight of (**f**) spleens and (**g**) livers ($n = 3$ mice/group, from one experiment; ns, not significant; two-way ANOVA with Tukey's multiple comparisons test). **h** Viable bacteria in the spleens and livers ($n = 3$ mice/group, from one experiment; *** $P = 0.0009$; ns, not significant; two-way ANOVA with Tukey's multiple comparisons test). **i** Plasmid loss in tumors colonized by SAM-FC ($n = 3$ mice/group, from one experiment; ns, not significant; two-way ANOVA with Tukey's multiple comparisons test). **j** Change in average body weight ($n = 10$ mice/group examined from two independent experimental replicates; ns, not significant; two-way ANOVA with Tukey's multiple comparisons test). **k-p** CT26 tumor-bearing mice were orally administered Doxy on day 0 or 3 after intravenous injection of SAM-FC (2×10^7 cfu). The levels of (**k**) aspartate aminotransferase (AST), (**l**) alanine transaminase (ALT), (**m**) blood urea nitrogen (BUN), (**n**) creatinine, (**o**) plasma C-reactive protein 2 (CRP2), and (**p**) procalcitonin (PCT) in serum were measured on day 5 ($n = 7$ mice/group examined from two independent experimental replicates, unpaired two-tailed *t*-test). Boxes represent the quartiles and whiskers mark the 10th and 90th percentiles. Yellow-shaded areas indicate the normal range of measured parameters.



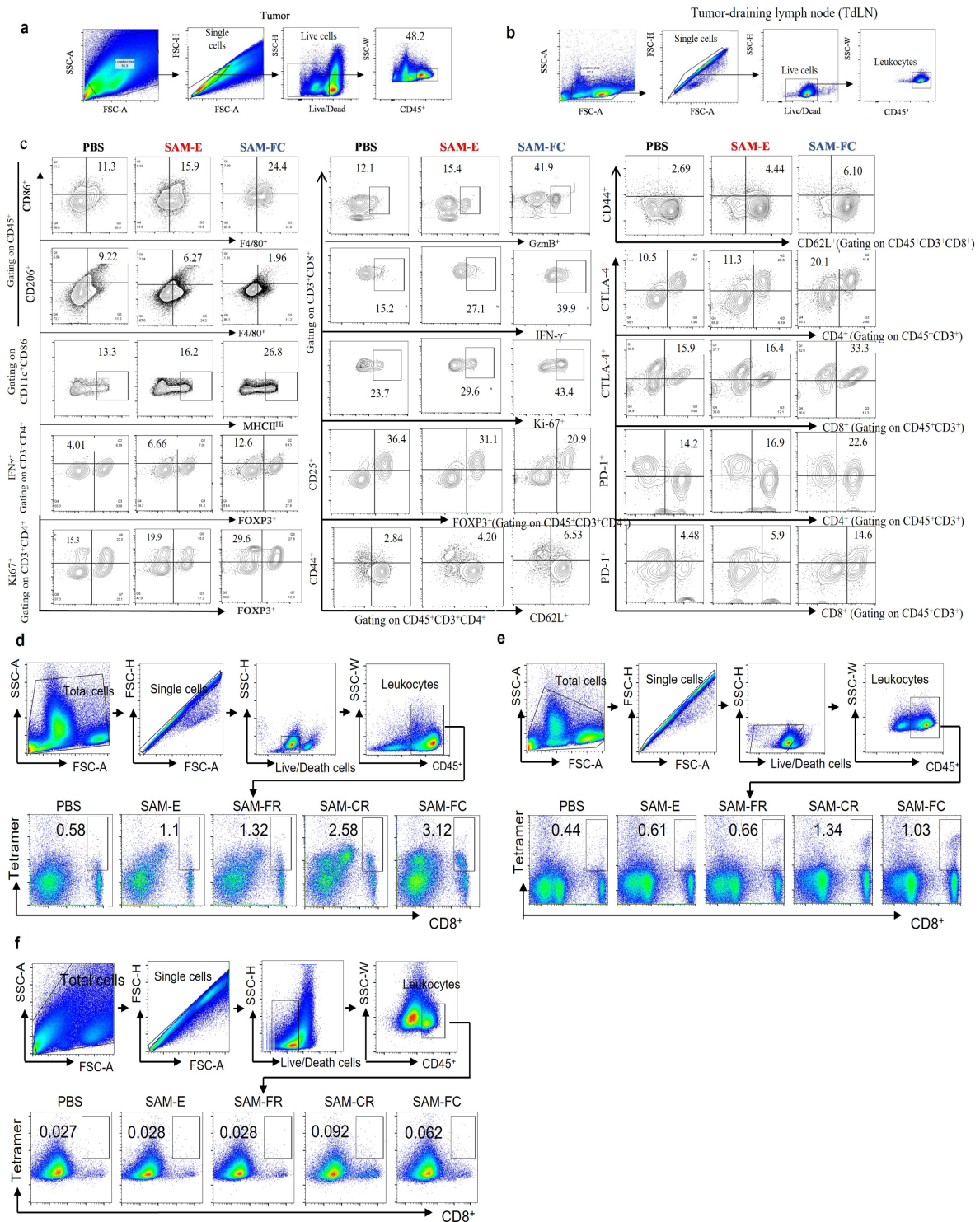
Supplementary Figure 4: Representative images of mice treated with SAM-FC and rechallenged mice (related to Fig. 1b-i). BALB/c or C57BL/6 mice were implanted subcutaneously with CT26 (1×10^6) or MC38 cells (5×10^5) into the hind right flank,

respectively. Then, the mice were treated with the indicated bacteria and sequentially with Doxy. PBS and SAM-E were used as treatment controls. The tumor-eradicated mice were rechallenged by subcutaneous implantation of the same tumor cells (2×10^6 for CT26 tumor-eradicated mice or 1×10^6 for MC38 tumor-eradicated mice) into the contralateral flank 90 days after initial tumor inoculation. Naïve, age-matched control mice. Rechallenge sites are marked by yellow arrows. **a** Representative images of CT26 tumor-bearing mice treated with engineered SAMs on day 0 – day 90, related to Fig. 1c, d. **b** Representative images of CT26 mice with primary tumor eradication after rechallenge with the same tumor cells, related to Fig. 1e. **c** Individual mouse tumor growth curves related to Fig. 1c, d. **d** Individual mouse tumor growth curves related to Fig. 1e. **e** Representative images of MC38 tumor-bearing mice treated with engineered SAMs on day 0 – day 90, related to Fig. 1g, h. **f** Representative images of MC38 mice with primary tumor eradication after rechallenge with the same tumor cells, related to Fig. 1i. **g** Individual mouse tumor growth curves related to Fig. 1g, **h** Individual mouse tumor growth curves related to Fig. 1i.

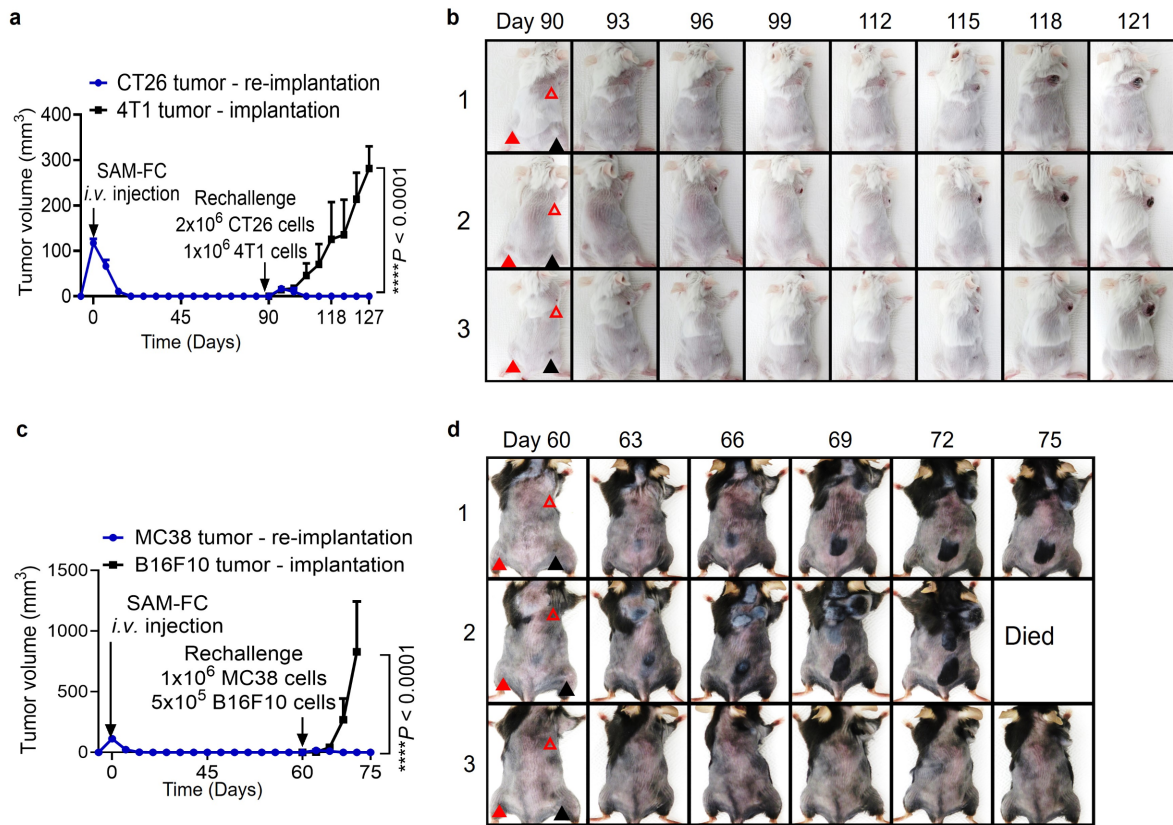


Supplementary Figure 5: Individual tumor images of the SAM-FC(+) group of CT26 tumor-bearing mice (related to Fig. 1c-e). **a** Images of the mice implanted with primary CT26 tumors ($n = 32$ mice examined from three independent experimental replicates). The mice with tumor eradication on day 90 are denoted by red numbers (24/32 mice, 75%). **b** Individual mouse images after secondary CT26 tumor rechallenge in the mice with primary tumor eradication. CT26 tumor cells were implanted subcutaneously into mice (left hind flank) that had no primary tumors by day 90 ($n = 16$ mice examined from two independent experimental replicates) and allowed to form secondary tumors. Mice without secondary tumor recurrence are denoted by red numbers (14/16 mice, 87.5%). Rechallenge sites are marked by yellow arrows.

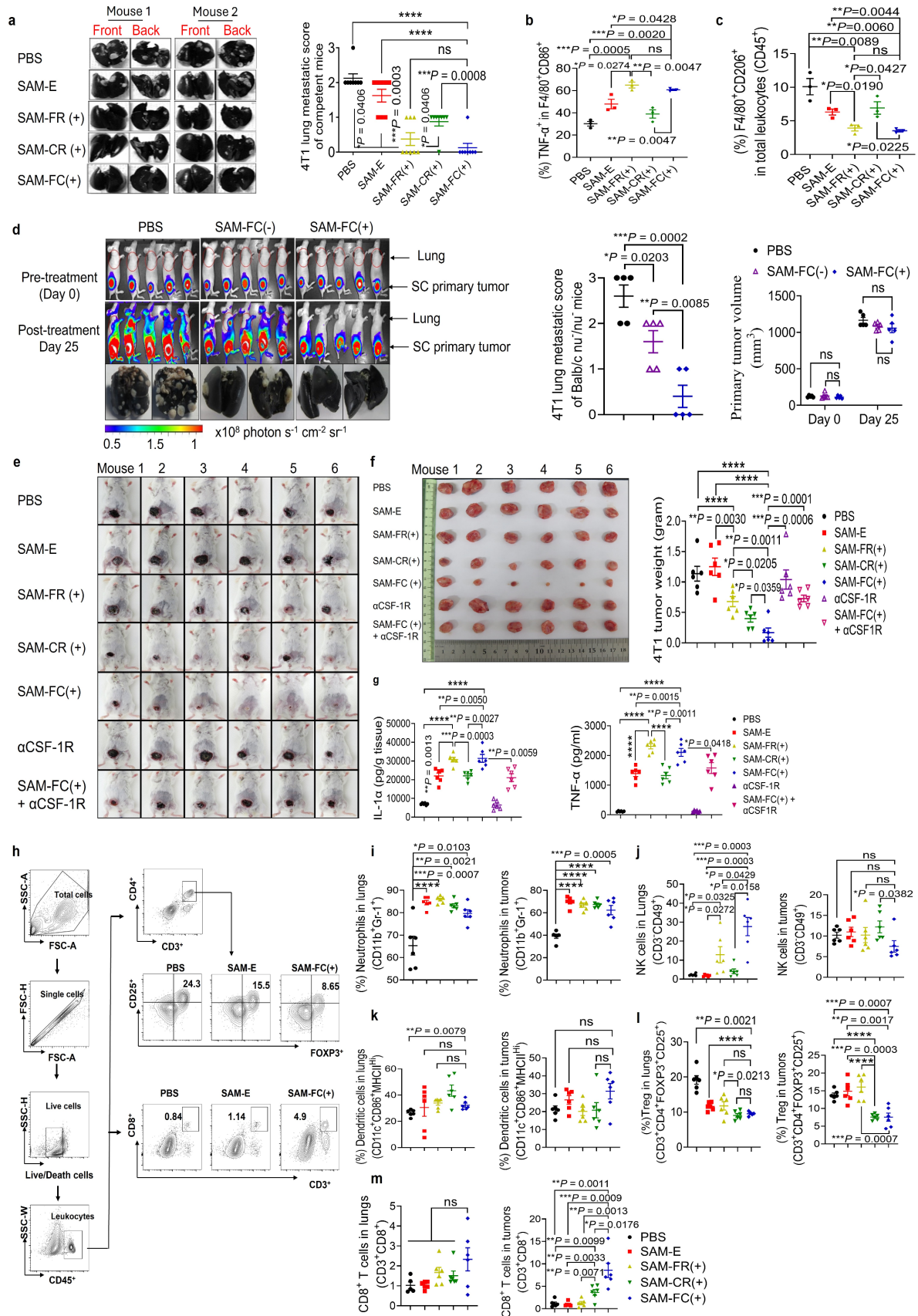
treated with Doxy. On day 9, tumors were obtained, and the immune cells were analyzed by flow cytometry. **a** Activated macrophages (IL-1 β ⁺CD11b⁺F4/80⁺) (n = 5 mice/group, from one experiment); **b** Neutrophils (CD11b⁺Gr-1⁺) (n = 5 mice/group, from one experiment); **c** Activated neutrophils (IL-1 β ⁺CD11b⁺Gr-1⁺) (n = 5 mice/group, from one experiment); **d** Activated DCs (IL-1 β ⁺CD11c⁺CD86⁺) (n = 5 mice/group, from one experiment); **e** Ki-67⁺CD4⁺FOXP3⁺ T cells (n = 7 mice/group examined from two independent experimental replicates); **f** Ki-67⁺CD8⁺ T cells (n = 7 mice/group examined from two independent experimental replicates); **g** IFN- γ ⁺CD8⁺ T cells (n = 5 mice, from one experiment); **h** CTLA-4⁺CD4⁺ T cells (n = 3 mice, from one experiment); **i** CTLA-4⁺CD8⁺ T cells (n = 3 mice/group, from one experiment); **j** PD-1⁺CD4⁺T cells (n = 3 mice/group, from one experiment). **** P < 0.0001; ns, not significant; unpaired two-tailed t -test. Please also see the flow cytometry gating strategies in Supplementary Fig. 7a-c. Immunofluorescence staining of tumor tissues for M2 and M1 macrophage markers, and for FOXP3, CD4, and CD8. **k** Tumor sections were double stained with antibodies for F4/80 (pink) and CD206 (green) (M2 macrophages); F4/80 (pink) and CD86 (green) (M1 macrophages); tumor sections single stained with antibodies for **(l)** FOXP3 (red); **(m)** CD4 (pink); **(n)** CD8 (yellow). Nuclei were stained with DAPI (blue). A merged image is shown at low (scale bars, 50 μ m) and high (scale bars, 20 μ m) magnification. **o-r** Cytokine profile of tumors treated with SAM bacteria. CT26 tumor-bearing mice were injected intravenously with the indicated bacteria and sequentially treated with Doxy, indicated by (+). On day 4, 6, and 9 after bacterial injection, tumors were excised and homogenized in protein extraction solution, and the levels of **(o)** IL-1 β , **(p)** TNF- α , **(q)** IFN- γ and **(r)** IL-4 in the supernatant were measured by ELISA (n = 5 mice/group, from one experiment; **** P < 0.0001; two-way ANOVA with Tukey's multiple comparisons test).



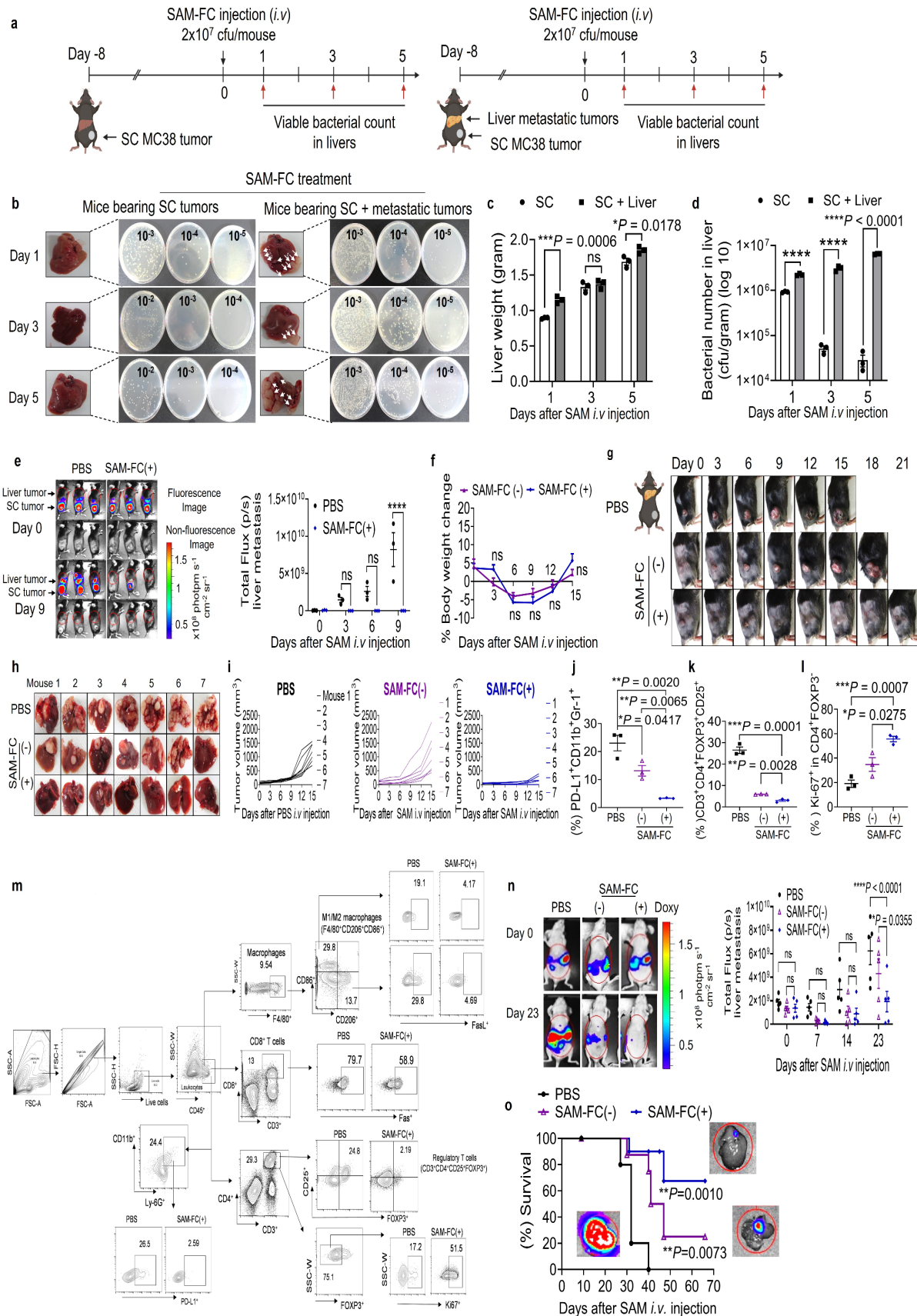
Supplementary Figure 7: Flow cytometry gating strategies (related to Fig. 2, Fig. 5, Fig. 6, and supplementary Fig. 6). Tumors, TdLNs, and peripheral blood were obtained from CT26 tumor-bearing mice after bacterial and Doxy treatment, and their immune cells were analyzed by flow cytometry. All samples were stained with the Live/Dead cell staining kit, an antibody against the CD45 hematopoietic cell maker, and specific immune cell markers. **a** Gating strategy used for the analysis of tumor samples. **b** Gating strategy for the analysis of TdLN samples. **c** Profiles of immune cells after gating. **d** Flow cytometry gating of Tet⁺ CD8⁺ T cells in peripheral blood. **e** Flow cytometry gating of Tet⁺ CD8⁺ T cells in TdLNs. **f** Flow cytometry gating of Tet⁺ CD8⁺ T cells in tumors.



Supplementary Figure 8: Anti-tumor-specific immunity generated by SAM-FC (related to Fig. 1e, and Fig. 2j, k). BALB/c or C57BL/6 mice were implanted with CT26 (1×10^6) or MC38 (5×10^5), respectively. SAM-FC were intravenously injected (day 0) and given Doxy (day3). The tumor-eradicated mice after SAM-FC(+) treatment were subcutaneously rechallenged with both CT26 and 4T1 tumor cells for CT26 tumor-eradicated mice or both MC38 and B16F10 tumor cells for MC38 tumor-eradicated mice, respectively, on the indicated days. **a** Average growth curves of the tumors in CT26 tumor-eradicated mice rechallenged with CT26 and 4T1 cells ($n = 3$ mice/group, from one experiment; **** $P < 0.0001$; two-way ANOVA with Tukey's multiple comparisons test). **b** Individual images of CT26 tumor-eradicated mice after rechallenge with CT26 and 4T1 tumor cells. Black triangles, primary CT26 tumors; filled red triangles, rechallenged CT26 tumors; open red triangles, rechallenged 4T1 tumors. **c** Average growth curves of tumors in MC38 tumor-eradicated mice after rechallenge with MC38 and B16F10 cells ($n = 3$ mice/group, from one experiment; **** $P < 0.0001$; two-way ANOVA with Tukey's multiple comparisons test). **d** Individual images of MC38 tumor-eradicated mice after rechallenge with MC38 and B16F10 cells. Black triangles, initial MC38 tumors; filled red triangles, rechallenged MC38 tumors; open red triangles, rechallenged B16F10 tumors.

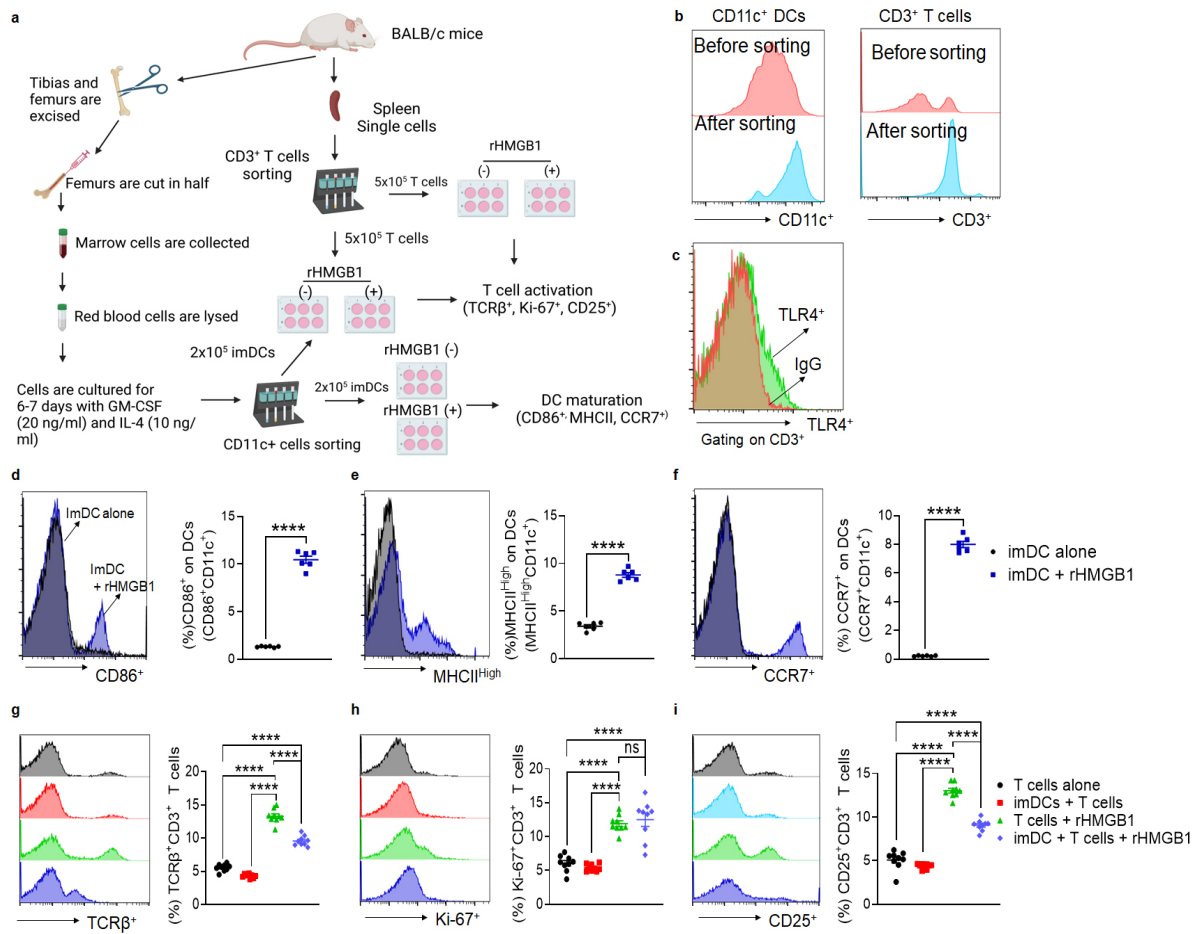


experimental replicates; **** $P < 0.0001$; ns, not significant; unpaired two-tailed t -test). Frequency of intratumoral **(b)** activated M1 (TNF α ⁺F4/80⁺CD86⁺) and **(c)** M2 (F4/80⁺CD206⁺) macrophages ($n = 3$ mice/group, from one experiment; ns, not significant; unpaired two-tailed t -test). **d** *In vivo* bioluminescent imaging and India ink staining of *ex vivo* lungs of 4T1-Luc2 tumor-bearing nude mice (left). The bioluminescent images of the mice were obtained on day 0 (pre-treatment) and day 25 (post-treatment). The lungs on day 25 were stained with India ink. 4T1-Luc2 metastatic nodules on the lung surface were counted and scored (middle). Subcutaneous 4T1-Luc2 primary tumors were also measured on day 25 (right) ($n = 5$ mice/group, from one experiment; ns, not significant; two-way ANOVA with Tukey's multiple comparisons test). **e** Individual images and **f** individual excised 4T1 tumors (left) and average tumor weight (right) of the mice bearing 4T1 tumors on the mammary fat pads on day 15 ($n = 6$ mice/group examined from two independent experimental replicates; **** $P < 0.0001$, ns, not significant; unpaired two-tailed t -test). **g** Tumor-localized inflammatory cytokines (IL-1 α and TNF- α) of the mice bearing 4T1 tumors on the mammary fat pads on day 6 ($n = 6$ mice/group examined from two independent experimental replicates; **** $P < 0.0001$; unpaired two-tailed t -test). **h** Flow cytometry gating of Treg and CD8⁺ T cells in lungs of the mice bearing 4T1 tumors on the mammary fat pads. **i-m** Frequency of immune cells in the mice bearing 4T1 tumors implanted into the mammary fat pad: **i** neutrophils (CD11b⁺Gr-1⁺) in lungs (left) and tumors (right); **j** NK (CD3⁺CD49⁺) in lungs (left) and tumors (right); **k** activated DCs (CD11c⁺CD86⁺MHCII^{hi}) in lungs (left) and tumors (right); **l** Treg (CD3⁺CD4⁺CD25⁺FOXP3⁺) in lungs (left) and tumors (right); **m** proliferating CD8⁺ T cells (CD3⁺CD8⁺) in lungs (left) and tumors (right) ($n = 6$ mice/group examined from two independent experimental replicates; ns, not significant; **** $P < 0.0001$; ns, not significant; unpaired two-tailed t -test).

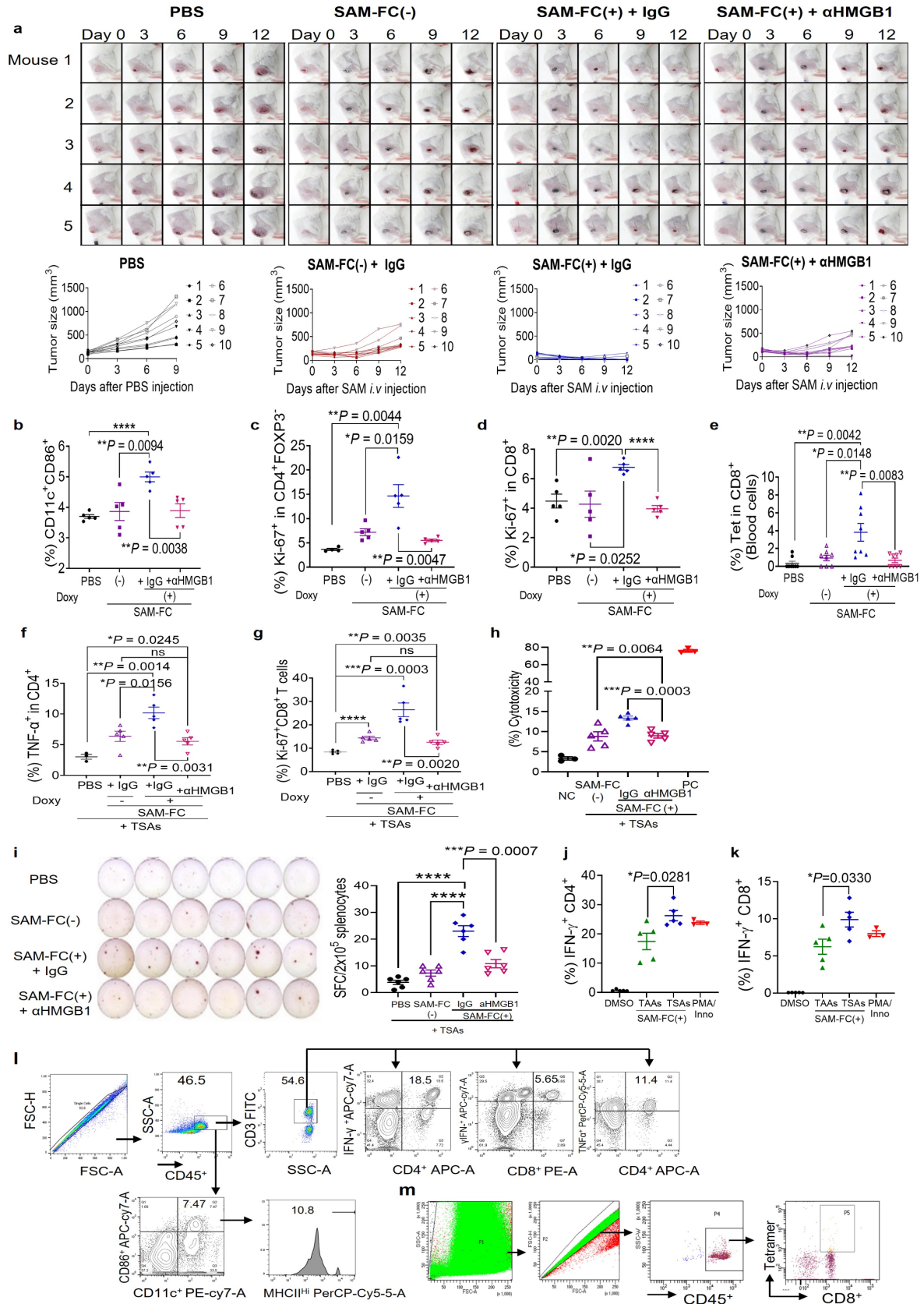


Supplementary Figure 10: Inhibition of lung and liver metastases by SAM-FC in different murine models (related to Fig. 3, h-k and Fig. 4). **a** Experimental scheme. **b** Representative liver images of the SC and SC + liver MC38 mice. **c** Liver weights

of SC and SC + liver MC38 mice ($n = 3$ mice/group, from one experiment; ns, not significant; two-way ANOVA with Tukey's multiple comparisons test). **d** SAM-FC counts in the livers of SC or SC + liver MC38 mice ($n = 3$ mice/group, from one experiment, **** $P < 0.0001$; two-way ANOVA with Tukey's multiple comparisons test). **e** *In vivo* bioluminescent imaging of SC + liver MC38-FLuc-RFP mice. Left, images; right, quantification of bioluminescent signals in the lungs ($n = 3$ mice/group, from one experiment, **** $P < 0.0001$; ns, not significant; two-way ANOVA with Tukey's multiple comparisons test). **f** Changes in average body weights in SC + liver MC38 mice. Body weight changes were calculated relative to those on day 0 ($n = 3$ mice/group, from one experiment; ns, not significant; two-way ANOVA with Tukey's multiple comparisons test). **g** Representative images of SC +liver MC38 mice. **h** Individual *ex vivo* images of the livers from SC +liver MC38 mice ($n = 7$ mice/group examined from 2 independent experimental replicates). **i** Individual growth curves of tumors in mice bearing SC + liver tumors treated with PBS, SAM-FC(-), or SAM-FC(+). **j-l** Frequencies of **(j)** hepatic PD-L1⁺CD11b⁺Gr-1⁺ neutrophils expressing PD-L1, **(k)** CD3⁺CD4⁺FOXP3⁺CD25⁺ Tregs, and **(l)** proliferating Ki-67⁺CD4⁺FOXP3⁺ T cells in mice treated as described in Fig. 4 ($n = 3$ mice/group, from one experiment; unpaired two-tailed *t*-test). **m** Gating strategy for the flow cytometry data in Fig. 4. **n** *In vivo* bioluminescent imaging of BALB/c athymic nu⁻/nu⁻ mice bearing intraperitoneal HepG2-FLuc tumors. The mice were implanted intraperitoneally with HepG2-FLuc cells. After 2 days, SAM-FC was injected intravenously (day 0), and then Doxy was given (day 3). Left, representative images; right, liver bioluminescence levels ($n = 5$ mice/group, from one experiment; ns, not significant; two-way ANOVA with Tukey's multiple comparisons test). **o** Kaplan-Meier survival curves from **(n)** [$n = 5$ mice/group, from one experiment; Log-rank (Mantel-Cox) test].

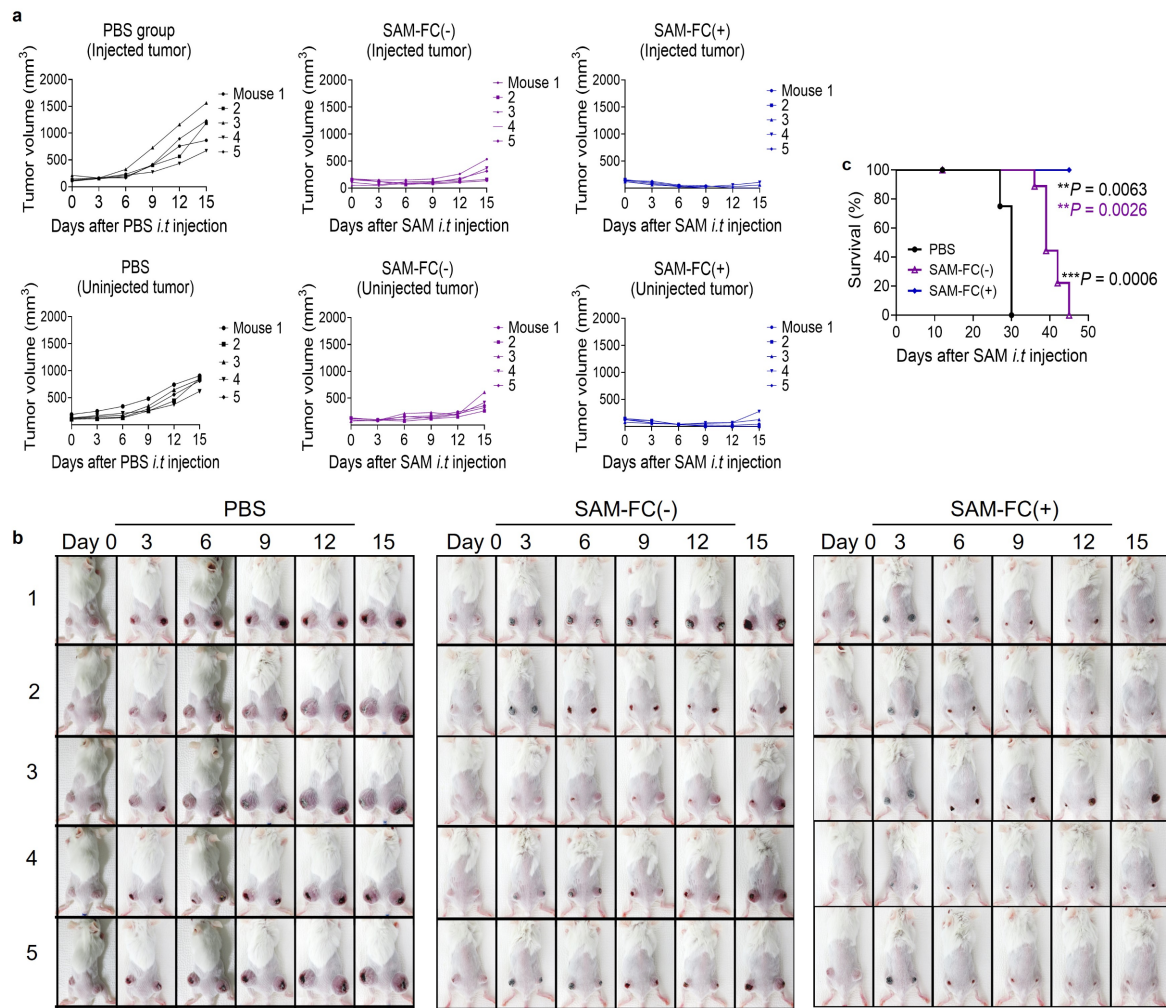


Supplementary Figure 11: Role of HMGB1 in DC maturation and T cell activation (related to Fig. 5.) **a** Experimental scheme. Immature DCs (imDCs; CD11c⁺) were isolated from the bone marrow (BM) of BALB/c using magnetic beads and co-cultured with 20 μ g/mL recombinant HMGB1 (rHMGB1). After 24h incubation, the matured DCs (CD86⁺MHCII^{High}CCR7⁺) were evaluated by flow cytometry. T cells (CD3⁺) were isolated from the spleens of the same mice by magnetic beads and the expression of Toll-like receptor 4 (TLR4) was evaluated. Then, CD11c⁺DCs (5×10^5) and CD3⁺ T cells (5×10^5) were co-cultured with or without rHMGB1 (20 μ g/mL). After 24h incubation, the activation of CD3⁺ T cells (TCRβ⁺Ki-67⁺CD25⁺) was measured by flow cytometry. **b** Cell populations before and after sorting of CD11c⁺DCs (left) and CD3⁺ T cells (right). **c** The expression of TLR4 in CD3⁺ T cells. **d-f** Frequency of mature DCs (CD86⁺CD11c⁺, MHCII^{High}CD11c⁺, CCR7⁺CD11c⁺). Left, histograms of CD86⁺ (d), MHCII^{High} (e), CCR7⁺ (f) after CD11c⁺ gating; right, quantitation of mDCs ($n = 6$ technical replicates; **** $P < 0.0001$; unpaired two-tailed t -test). Frequency of TCRβ⁺ (g), proliferating Ki-67⁺ (h), and CD25⁺ (i) in CD3⁺ T cells (Left, histograms; right, quantification) ($n = 9$ technical replicates, **** $P < 0.0001$; ns, not significant; unpaired two-tailed t -test.) All data are shown as mean \pm s.e.m.



treatment and used either for flow cytometry analysis (b-e) or co-cultured with CT26 cancer cells (h) or TAA/TSA peptides (f-k).

a Representative image (upper) and individual tumor growth curves (lower) related to data shown in Fig. 5a, b ($n = 10$ mice/group examined from two independent experimental replicates). Frequency of **(b)** DCs (CD11c⁺CD86⁺), **(c)** proliferating CD4⁺ T (Ki-67⁺CD4⁺FOXP3⁻) cells, **(d)** proliferating conventional CD8⁺ T (Ki-67⁺CD8⁺) cells in spleens ($n = 5$ mice/group from one experiment; **** $P < 0.0001$; unpaired two-tailed t -test). **e** Frequency of tumor specific CD8⁺ T (Tet⁺CD8⁺) cells in peripheral blood ($n = 8$ mice/group examined from two independent experimental replicates; **** $P < 0.0001$; unpaired two-tailed t -test). Flow cytometry quantification of splenic **(f)** TNF- α ⁺CD4⁺ T cells and **(g)** Ki-67⁺CD8⁺ T cells against TSA peptides ($n = 5$ mice/group, from one experiment; ns, not significant; unpaired two-tailed t -test). The same samples described in f and g were co-cultured for 6 h with CT26 cancer cells at a 1:1 ratio. **h** Cytotoxicity was measured using the LDH activity assay ($n = 5$ mice/group, from one experiment; unpaired two-tailed t -test). NC, negative control (untreated tumor cells); PC, positive control (tumor cells treated with lysis buffer). T cell responses against TSA peptides within the SAM-FC-treated splenocyte population were measured in an IFN- γ ELISpot assay using the splenocyte populations shown in **(i)** (left) and the spot-forming cells (SFC) were counted (right) ($n = 6$ mice/group, from one experiment; **** $P < 0.0001$; unpaired two-tailed t -test). **j** Activation of CD4⁺ T cells (IFN- γ ⁺ CD4⁺) and **k** CD8⁺ T cells (IFN- γ ⁺ CD8⁺) by TAA and TSA peptides within the total population of SAM-FC-treated splenocytes ($n = 5$ mice/group, from one experiment; unpaired two-tailed t -test). **l** Gating strategy for flow cytometry analysis related to Fig. 5i-m. **m** Gating strategy for tumor-specific Tet⁺ CD8⁺ T cells corresponding to the data shown in (e).



Supplementary Figure 13: Individual tumor growth curves and survival rates of dual CT26 tumor-bearing mice after intratumoral SAM-FC treatment (related to Fig. 6d). **a** Individual growth curves of bacteria-injected and untreated distal tumors ($n = 5$ mice/group, from one experiment). **b** Individual mouse images relating to the data shown in (a); bacteria were injected into the tumors on the left flank. **c** Kaplan-Meier survival curves ($n = 5$ mice/group, from one experiment; $**P = 0.0063$ [SAM-FC(+) vs PBS], $**P = 0.0026$ [SAM-FC(+) vs SAM-FC(-)], $***P = 0.0006$ [SAM-FC(-) vs PBS]; Log-rank (Mantel-Cox) test) corresponding to the data shown in (a).

Supplementary Table 1: List of primers used in the study

Primer name	Sequence	Remarks	Company
FlaB-P _{tetA} -F(StuI)	5'-CATCACGTTGTCAGAGCGCATGTCT-3'	Plasmid construction	Macrogen, Korea
FlaB-P _{tetA} -R(SacI)	5'- AGACATGCGCTCTGACAACGTGATG -3'		
ClyA-P _{tetA} -F(StuI)	5'-AAAGGCCTTCCGTTTTTTGGGCTAACAGGAGGAAT-3'		
ClyA-P _{tetA} -R(SacI)	5'-TTTGAGCTCGTCGACTCAGACGTCAGGAACCTCGAAAAGC-3'		
ClyA-P _{tetR} -F(KpnI)	5'- TATAGGCCTATGACCGGAATATTTGCAGAACAAACTGTAGAG		
ClyA-P _{tetR} -R(SalI)	5'- TTTGAGCTCGCATGCTCAGACGTCAGGAACCTCGAAAAGC		
Rluc8-P _{tetR} -F(KpnI)	5'- AAAGGTACCATGGCTTCCAAGGTGTAC		
Rluc8-P _{tetR} -R(HindIII)	5'- TTAAAGCTTTTACTGCTCGTTCTTCAGCACGC		

Supplementary Table 2: Plasmid and bacteria strains used in this study
(A) Bacterial strains

Strain	Genotype	Purpose
<i>S. typhimurium</i>	Δ ppGpp (Δ relA, Δ spoT)	Attenuated <i>S. typhimurium</i>
<i>E. coli</i> DH10-beta	Δ (ara-leu) 7697 araD139 fhuA Δ lacX74 galK16 galE15 e14- ϕ 80dlacZ Δ M15 recA1 relA1 endA1 nupG rpsL (Str ^R) rph spoT1 Δ (mrr-hsdRMS-mcrBC)	Cloning and amplification of plasmids

(B) Plasmids

Plasmid	Construct	Antibiotic resistance	References
pBAD-ClyA	<i>clyA</i> under the control of P_{BAD} promoter	Ampicillin	33
pBAD-FlaB	<i>FlaB</i> under the control of P_{BAD} promoter	Ampicillin	32
pBAD-Rluc8	<i>Rluc8</i> under the control of P_{BAD} promoter	Ampicillin	33
pJH18	Backbone	Ampicillin	36
pJH18-FR	<i>FlaB</i> under the control of P_{tetA} promoter, <i>Rluc8</i> under the control of P_{tetR} promoter	Ampicillin	This study
pJH18-CR	ClyA under the control of P_{tetA} promoter, <i>Rluc8</i> under the control of P_{tetR} promoter	Ampicillin	This study
pJH18-FC	<i>FlaB</i> under the control of P_{tetA} promoter, <i>ClyA</i> under the control of P_{tetR} promoter	Ampicillin	This study

Supplementary Table 3: CDI values of SAM-FC(+) treatment in CT26 and MC38 tumor models

Average tumor volume (mm ³)	Control (SAM-E)	A [SAM-FR(+)]	B [SAM-CR(+)]	AB [SAM-FC(+)]	CDI	Interpretation
CT26 tumor model (day 15)	555.5	383.05	224.05	53.19	0.34	Synergism
MC38 tumor model (day 12)	476.33	63	496.7	60.87	0.93	Synergism

CDI, coefficient of drug interaction; $CDI = \{(AB/control)/[(A/control) \times (B/control)]\}$

Supplementary Table 4: Peptide tumor-associated antigens and neoantigens used in this study⁴

Protein source	TAA (wildtype)	NeoAg
Aldh18a1	HSGQNHLKEMAIPVLEARACAAAGQ	HSGQNHLKEMAI <u>S</u> VLEARACAAAGQ
E2f8	ILPQAPSGPSYAIYLQPAQAQMLTP	ILPQAPSGPSYA <u>T</u> YLQPAQAQMLTP
Mtch1	SWIHCWKYLSVQGSQ ^L FRGSSLLFRR	SWIHCWKYLSVQ <u>S</u> SQ ^L FRGSSLLFRR
Glud1	LRTAAYVNAIEKVF ^K VYNEAGVTFT	LRTAAYVNAIEK <u>I</u> F ^K VYNEAGVTFT

TAA, tumor-associated antigen; NeoAg, neoantigen. Mutated amino acids are highlighted in bold and underlined.

Supplementary Table 5: Antibodies used in this study.

Ab ID	Ab description	Manufacturer/Catalogue number	Application
Rabbit anti-TetR Antibody	Polyclonal Ab	Novusbio/NB600-234	Western blotting
Rabbit anti-ClyA	Polyclonal Ab	Lab preparation	
HRP-conjugated rabbit anti-mouse immunoglobulins	Polyclonal Ab	Dako/P0260	
HRP-conjugated goat anti-rabbit immunoglobulins	Polyclonal Ab	Dako/P0448	
Rabbit anti-FlaB	Polyclonal Ab	A gift from Dr. Joon Haeng Rhee, Chonnam National University Medical School (32)	
Rabbit anti-ALDH18A1	Polyclonal Ab	Novus Biologicals/NBP1-83324	
Rabbit anti-Mtch1	Polyclonal Ab	Novus Biologicals/NBP1-69285	
Rabbit anti-E2F8	Polyclonal Ab	Abcam/ab109596	
Rabbit anti-GluD1	Polyclonal Ab	Thermo Fisher Scientific /PA5-28301	
Anti Rabbit β -actin	Clone 13E5	Cell Signalling/4970L	
Goat anti-rabbit IgG H & L (HRP)	Polyclonal Ab	Abcam/ab205718	ELISA
IL-12 p70 mouse uncoated ELISA kit with plates	Specific monoclonal Ab	Thermo Fisher Scientific /88-7121-22	
IL-1 β Mouse Uncoated ELISA Kit with Plates	Specific monoclonal Ab	Thermo Fisher Scientific /88-7013-22	
TNF α Mouse Elisa Kit, High Sensitivity	Specific monoclonal Ab	Thermo Fisher Scientific /BMS607HS	
IFN- γ mouse ELISA Kit	Specific monoclonal Ab	Invitrogen/BMS606	
IL-4 mouse ELISA Kit	Specific monoclonal Ab	Invitrogen/BMS606	
Mouse IFN- γ T-cell ELISpot Kit	Specific monoclonal Ab	U-CyTech/CT317-PB5	
Anti-mouse CD16/32	TruStain FcX™ Fc blocking	BioLegend/101320	Flow cytometry
Live/dead Fixable aqua dead cell stain kit		Invitrogen/L34957	

Anti-TLR5-Alexa Fluor 488	Clone 19D579.2	IMGENEX/IMG-664AF488
PE anti-mouse TLR4 (CD284)/MD2 Complex Antibody (clone MTS510)	Clone MTS510	BioLegend/117606
PE Rat IgG2a, κ Isotype Ctrl Antibody	Clone RTK2758	BioLegend/400508
PE anti-mouse TCR β chain Antibody	Clone H57-597	BioLegend/109208
PE Armenian Hamster IgG Isotype Ctrl Antibody	Clone HTK888	Biolegend/400908
Anti-mouse CD197 (CCR7)- PE	Clone 4B12	eBioscience/12-1971-82
Rabbit anti-calreticulin	Clone D3E6	Cell Signaling Technology/12238S
Anti-rabbit IgG (H & L)		Cell Signaling Technology/4412S
Rabbit (DA1E) mAb IgG	Clone DA1E	Cell Signaling/#3900S
Anti-mouse CD45.2-Pacific blue	Clone 104	BioLegend/109820
Anti-mouse CD3-FITC	Clone 17A2	eBioscience/11-0032-82
Anti-mouse CD11c-FITC	Clone N418	eBioscience/11-0114-82
Anti-mouse 11b-FITC	Clone M1/70	BioLegend/101205
Anti-mouse CD4-APC	Clone GK1.5	BioLegend/100412
Anti-mouse CD8a-PE	Clone 53-6.7	eBioscience/12-0081-82
Anti-mouse CD274-PE	Clone 10F.9G2	BioLegend/12-0081-82
Anti-mouse F4/80-PE	Clone BM8	eBioscience/124801-82
Anti-mouse IL-1 β PE	Clone CRM56	eBioscience/12-7018-82
Anti-mouse CD86-PE	Clone GL1	eBioscience/12-0862-82

Anti-mouse CD49-PE	Clone DX5	BioLegend/108908
Anti-mouse FOXP3-APC	Clone FJK-16s	eBioscience/77-5775-40
Anti-mouse CD49-APC	Clone DX5	BioLegend/108909
Anti-mouse CD4-APC	Clone GK1.5	BioLegend/100412
Anti-mouse Gr-1-APC	Clone 1A8	BioLegend/127614
Anti-mouse CD274-APC	Clone B7-H1	BioLegend/124312
Anti-mouse CD206-APC	Clone B7-H1	BioLegend/C068C2
Anti-mouse CD25-PerCP-Cy5.5	Clone PC61	BioLegend/102030
Anti-mouse CD279-PerCP-Cy5.5	Clone RMP130	BioLegend/109120
Anti-mouse granzyme B-PerCP-Cy5.5	Clone QA16A02	BioLegend/372212
Anti-mouse CD8-PerCP-Cy5.5	Clone 53-6.7	BioLegend/100733
Anti-mouse CD62L-PerCP-Cy5.5	Clone MEL-14	BioLegend/104432
Anti-mouse MHCII-PerCP-Cy5.5	Clone M5/114.15.2	BioLegend/107625
Anti-mouse Ly-6G-PerCP-Cy5.5	Clone RB6-8C5	BioLegend/127615
Anti-mouse F4/80-PerCP-Cy5.5	Clone BM8	BioLegend/123128
Anti-mouse Ki67-PE-Cy7	Clone SolA15	Thermo Fisher Scientific/25469882
Anti-mouse CD152-PE-Cy7	Clone UC10-4B9	BioLegend/106313
Anti-mouse CD8 PE-Cy7	Clone 53-6.7	eBioscience/25-0081-82
Anti-mouse CD206 PE-Cy7	Clone C068C2	BioLegend/141719
Anti-mouse CD11c PE-Cy7	Clone N418	Thermo Fisher Scientific/25-0114-82

Anti-mouse IFN γ -APC-Cy7	Clone XMG1.2	BioLegend/505849	
Anti-mouse PD-1-APC-Cy7	Clone 29F.1A12	BioLegend/135224	
Anti-mouse CD44-APC-Cy7	Clone IM7	BioLegend/103028	
Anti-mouse CD86-APC-Cy7	Clone GL-1	BioLegend/105029	
H-2Ld MuLV gp70 Tetramer-SPSYVYHQF-APC	Allele: H-2Ld	MBL/TB-M521-2	
Anti-mouse CD4	Clone GK1.5	Bio X Cell/BP0003-1	CD4 ⁺ T depletion
Anti-mouse CD8 α	Clone 2.43	Bio X Cell/BP0061	CD8 ⁺ T depletion
Rat IgG2b isotype control Ab	Clone LTF-1	Bio X Cell/BP0090	T-cell depletion control
InVivoMAb anti-mouse CSF1R (CD115)	Clone AFS98	Bio X Cell/BE0213	Macrophage depletion
<i>InVivo</i> MAb rat IgG2a isotype control, anti-trinitrophenol	Clone 2A3	Bio X Cell/BE0089	Macrophage depletion control
Anti-HMGB1, ChIP grade	Polyclonal Ab	Abcam/ab18256	HMGB1 neutralization, Western blotting
Rabbit IgG, ChIP grade	Polyclonal Ab	Abcam/ab171870	HMGB1 neutralization control

Ab, antibody; HRP, horseradish peroxidase, ELISA, Enzyme-linked immunosorbent assay.